# Integrated GWAS, linkage, and transcriptome analysis to identify genetic loci and candidate genes for photoperiod sensitivity in maize

Yulin Jiang[1,2†], Shuang Guo[1,3†], Dong Wang[1,3†], Liang Tu[1†], Pengfei Liu[1†], Xiangyang Guo[1†], Angui Wang[1], Yunfang Zhu[1†], Xuefeng Lu[1,2†], Zehui Chen[1*†] and Xun Wu[1,2*†]

[1]Institute of Upland Food Crops, Guizhou Academy of Agricultural Sciences, Guiyang, Guizhou, China, [2]Ministry of Agriculture and Rural Affairs Key Laboratory of Crop Genetic Resources and Germplasm Innovation in Karst Region, Guiyang, China, [3]College of Agriculture, Guizhou University, Guiyang, China

**Introduction:** Maize photosensitivity and the control of flowering not only are important for reproduction, but also play pivotal roles in the processes of domestication and environmental adaptation, especially involving the utilization strategy of tropical maize in high-latitude regions.

**Methods:** In this study, we used a linkage mapping population and an inbred association panel with the photoperiod sensitivity index (PSI) phenotyped under different environments and performed transcriptome analysis of T32 and QR273 between long-day and short-day conditions.

**Results:** The results showed that PSIs of days to tasseling (DTT), days to pollen shedding (DTP), and days to silking (DTS) indicated efficacious interactions with photoperiod sensitivity for maize latitude adaptation. A total of 48 quantitative trait loci (QTLs) and 252 quantitative trait nucleotides (QTNs) were detected using the linkage population and the inbred association panel. Thirteen candidate genes were identified by combining the genome-wide association study (GWAS) approach, linkage analysis, and transcriptome analysis, wherein five critical candidate genes, *MYB163*, *bif1*, *burp8*, *CADR3*, and *Zm00001d050238*, were significantly associated with photoperiod sensitivity.

**Discussion:** These results would provide much more abundant theoretical proofs to reveal the genetic basis of photoperiod sensitivity, which would be helpful to understand the genetic changes during domestication and improvement and contribute to reducing the barriers to use of tropical germplasm.

# 1 Introduction

Maize (*Zea mays* L.) originated in southern Mexico and has spread over a wide latitudinal range. In the process of expansion from tropical to temperate regions, maize germplasm has necessitated a reduction of its photoperiod sensitivity in adaptation to local environments (Edmeades et al., 2017). In southwest China, the resistance to diseases and insect pests was the most significant factor affecting maize production (https://www.stats.gov.cn/). The tropical maize germplasm was widely used during breeding practice, and the heterotic pattern of "temperate × tropical" played an important role in this region. However, tropical maize germplasms always showed stronger photoperiod sensitivity when planted under long-day (LD) environments, i.e., foundation inbred of T32 derived from tropical maize germplasms. Therefore, the photoperiod sensitivity characterization and relevant candidate genes are beneficial to major maize tropical germplasm improvement and seed production.

Most maize varieties are short-day (SD) plants, especially tropical germplasm, and the difference in photoperiod sensitivity largely reflects the responses of crop germplasm ecotypes with LD conditions (Birch et al., 1998; Khotasena et al., 2022). The photoperiod sensitivity index (PSI) could be a representative trait, which showed the stage of the plant to be affected by light length change from the vegetative to the reproductive stage. The specific calculation method is PSI = ± (average value of a trait under long day/average value under short day)/average value under short day (Zhang et al., 2011). Appropriate trait measurements are necessary to efficaciously appraise photoperiod sensitivity. Days to tasseling (DTT), days to pollen shedding (DTP), and days to silking (DTS) were successfully introduced for PSI consideration (Zhang et al., 2011; Khotasena et al., 2022; Wu et al., 2023). The leaf number (LN), plant height (PH), and ear height (EH) before the reproductive phase change are determined largely by the rate and pattern of leaf initiation during vegetative development and the duration of the vegetative phase controlled by the timing of floral transition (Langdale, 2005; Colasanti and Muszynski, 2009).

Several studies have detected quantitative trait loci (QTLs) for photoperiod sensitivity by using linkage analysis and association mapping. Li et al. (2016a) conducted a comprehensive genetic dissection to assess the genetic architecture of LN and its genetic relationship to flowering time, using a large set of 866 maize-teosinte $BC_2S_3$ recombinant inbred lines, and validated the pleiotropy of the genes *ZCN8*, *dlf1*, and *CCT* on LN and flowering. Li et al. (2016b) identified a total of 90 flowering time-related regions, found nearly 1,000 flowering time-associated single-nucleotide polymorphisms (SNPs), and mainly distributed approximately 220 candidate genes, by using the parallel linkage analysis of two NAM panels with more than 8,000 lines. Du et al. (2023) found a unique QTL *qPss3* by using two segregating populations that behaved as a dominant locus and caused earlier flowering by 2–4 days via inhibiting *ZmCCT10*-induced photoperiod sensitivity under LD conditions. Fei et al. (2022) identified 39 QTLs and explored four candidate genes (*Zm00001d006212*, *Zm00001d017241*, *Zm00001d047761*, and *Zm00001d047632*) enriched in the plant circadian rhythm

pathway in the consensus major QTL region via combined analysis of transcriptome data. Wu et al. (2023) identified 25 important candidate genes for maize flowering time by integrating genome-wide association study (GWAS), linkage analysis, and transcriptome analysis. In conclusion, combining the method with linkage analysis and GWAS identified hundreds of candidate genes that may smash in the negative limitations of photosensitivity, thus contributing to the large-scale environmental adaptation of maize to altitude and latitude, such as *Vgt1*, *RAP2.7*, *Ghd7*, *D8*, *PHYC1/2/3*, *CCA1*, *Floridalma/Leafy 1/2*, *bif2*, CCTs, ZCNs, ZMMs, ELFs, and PRRs, to name a few (Xu et al., 2012; Wang et al., 2019; Zhao et al., 2023). It is worth noting that previous reports for photoperiod sensitivity aimed at flowering time, but few about PSI based on the values in different photoperiodic environments. These indirect traits, thermal time or PSI, have also true interactions with photoperiod sensitivity under LD or both LD and SD photoperiod environments (Xu et al., 2012).

In this study, we used a linkage mapping population with 150 $F_{2:3}$ offspring obtained from the cross derived from the inbred lines T32 and QR273, and one natural association panel with 226 inbred lines to be materials, and proceeded PSI phenotyping under different photoperiod environments. Based on this, GWAS and linkage analysis were performed. After that, transcriptome data of T32 and QR273 were also determined between LD and SD conditions. Finally, QTL/quantitative trait nucleotides (QTNs) and relevant candidate genes for PSI of DTT, DTP, and DTS were identified. These results would help to provide some new proof for exploring the genomic basis of PSI in tropical maize germplasm.

# 2 Materials and methods

## 2.1 Plant materials and field experiments

An association mapping panel with 226 inbred lines and a linkage population with 150 $F_2$ and $F_{2:3}$ offspring derived from the cross between maize foundation inbred lines of QR273 and T32 were chosen in this study. Both foundation parents of QR273 and T32 were derived from the Suwan population. T32 was delayed in flowering and even failed to flower when planted under LD conditions, which showed a strong photoperiod sensitivity characteristic; on the contrary, QR273 bloomed normally (Wu et al., 2023). These materials were planted in Zhangye (ZY 38.93° N, 100.45°E, Gansu Province) for the strongest LD condition with an approximately 15-h/9-h photoperiod, Guiyang (GY 26.5°N, 106.7°E, Guizhou Province) for the mid-LD condition with a 13-h/11-h photoperiod, and Sanya (SY 18.36°N, 109.16°E, Hainan Province) for the SD condition with an approximately 12-h/12-h photoperiod. Meanwhile, the linkage population with $F_2$ lines and the foundation parents QR273 and T32 were planted in SY for genotyping, and then $F_{2:3}$ offspring and parent lines were planted in ZY and SY for phenotyping, respectively. A randomized complete block design was selected for field experiments, in which each line was planted in a single row, with a 3-m row length, with 12 individual plants in one row, and with an 80-cm space between

rows. Field management including fertilization, irrigation, pest, and weed control was carried out based on local practices.

## 2.2 Photoperiod sensitivity index evaluation

LN, PH, EH, and three flowering time-related traits (DTT, DTS, and DTP) were chosen for PSI analysis. LN, PH, and EH were measured after the end of pollination. DTT, DTS, and DTP represent the number of days from sowing to the time when 50% of plants of each line exhibited the corresponding traits. PSI was calculated according to the method described by Fei et al. (2022): PSI = [(average value of the trait in long day − average value of the trait in short day)/average value of the trait in short day × 100%]. The PSI could be graded into four levels, in which <0% PSIs are classified as tolerant to the photoperiod, 0%–30% PSIs are identified as insensitive to the photoperiod, 31%–70% PSIs are considered as weakly sensitive to the photoperiod, and more than 71% PSIs are categorized as strongly photoperiod sensitive (Khotasena et al., 2022).

## 2.3 DNA extraction and genotyping

Leaf samples for DNA extraction were pooled from five plants in each line and collected from the five-leaf stage of maize seedlings. DNA extraction was performed according to the method following Saghai-Maroof et al. (1984). The association panel lines were genotyped using MaizeSNP50 BeadChip containing 56,110 SNPs, and this work was already done as described by Wu et al. (2019). Regarding linkage population lines, DNA quality testing and genotyping by sequencing (GBS) assessments were completed by the Beijing Compass Biotechnology Company, and the detailed methods followed the description by Wu et al. (2023).

## 2.4 Genome-wide association study and QTL mapping

The inbred association panel was utilized to perform a GWAS as described by Wang et al. (2023). Briefly, a total of 43,252 SNPs were used to perform a phenotype–genotype GWAS by using the TASSEL v5.2.80 software with a mixed linear model (MLM) and log10($p$) threshold ≥4.0. The population structure and pairwise kinship were treated as covariates. Regarding the $F_{2:3}$ population, after filtering SNPs with minor allele frequency (MAF < 0.05), we obtained a total of 68,994 high-quality SNPs that were used for the genetic map building. QTL mapping analyses were performed by using the QTL IciMapping software Version 4.1 (Wu et al., 2023). The positive correlations were detected by $r > 0.8$, $p < 0.05$.

## 2.5 Transcriptome analysis

The parent lines T32 and QR273 were grown at experiment fields of ZY and SY as described above. Leaf tissues were separated and pooled from three plants per line at the maize nine-leaf stage (V9) with three experimental repeats. Fresh tissues were immediately frozen in liquid nitrogen and stored at −80℃ before RNA isolation. Total RNA was extracted using TRIzol (Invitrogen, Carlsbad, USA) according to the method by Gehrig et al. (2000). The cDNA synthesis and RNA sequencing were finished using the Illumina HiSeq 2000 platform at Biomarker Technologies Company (Beijing, China). The transcriptome data were analyzed as described by Wu et al. (2023).

## 2.6 Candidate gene prediction and verification

Functional annotations of these candidate genes were performed by using online search tools (https://www.maizegdb.org/). Quantitative reverse transcription polymerase chain reaction (qRT-PCR) analysis was performed as described by Jiang et al. (2021). The qRT-PCR primers were designed by the online PrimerQuest Tool (https://www.idtdna.com/Primerquest/Home/Index). ACTIN and GAPDH genes were used to normalize the expression of genes. The fold difference ($2^{-\Delta\Delta Ct}$) and relative quantities were calculated using the CFX Manager Software version 3.1 (Bio-Rad, Hercules, USA).

## 2.7 Statistical analysis

Statistical analyses of experimental data were performed using the Student's $t$-test (*$p < 0.05$, **$p < 0.01$, ***$p < 0.001$) by the software of IBM SPSS Statistics v22 (International Business Machines Corporation, New York, USA).

# 3 Results

## 3.1 PSI variation under different environments

The tropical maize lines generally exhibit growth defects, such as delayed tasseling and silking, inconsistency between male and female, and yield decline when they are transplanted to high-latitude areas because of the high sensitivity characteristic to LD conditions. In this study, the foundation parental line T32 derived from the tropical germplasm of the Suwan population delayed tasseling, pollen shedding, and silking by approximately 54, 65, and 67 days, respectively, when it was grown at ZY (LD condition) compared to SY (SD condition). In addition, T32 also showed higher PH and EH, and more leaves (Figure 1A), but extremely fewer kernels (Figure 1B) when it was planted under LD conditions. Correspondingly, PSIs of DTT, DTP, DTS, PH, and EH for T32 were more than 71%, which indicated that these traits were highly associated with photoperiod sensitivity (Figure 1C). Although the foundation parental line QR273 also showed delayed flowering time-related traits under LD conditions when compared to those under SD conditions, PSIs of these traits were statistically lower and showed that such traits had weak or no photoperiod sensitivity (Figure 1C). After that, we analyzed the PSI of T32 and QR273, their
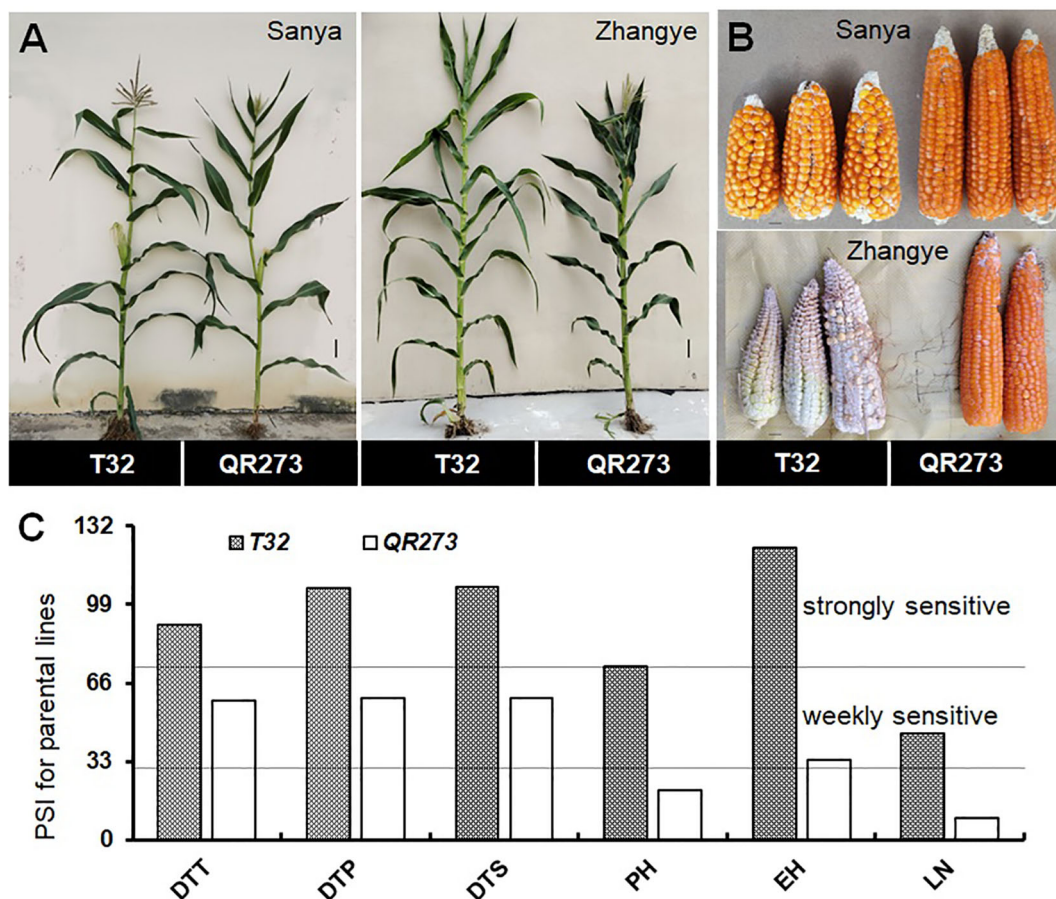
**FIGURE 1**
Linkage analysis for the photoperiod sensitivity index (PSI) of days to tasseling (DTT), days to pollen shedding (DTP), and days to silking (DTS), the leaf number (LN), plant height (PH), and ear height (EH) in the $F_{2:3}$ population. The plant **(A)** and ear **(B)** phenotypes of the parental lines, T32 and QR273, in the different latitude areas (Sanya and Zhangye). **(C)** The PSI distribution of flowering time traits, PH, EH, and LN in the $F_{2:3}$ population at the Sanya and Zhangye.

$F_2$ and $F_{2:3}$ offspring, and an association panel planted under three different latitude areas with ~15 h/9 h (ZY), 13.5 h/10.5 h (GY), and 12 h/12 h (SY) photoperiods. Results showed that PSIs of most traits for SY/ZY showed a higher sensitivity for T32 and relevant $F_{2:3}$ family lines, but a lower sensitivity for SY/GY and GY/ZY (Table 1). Additionally, PSIs of DTT, DTP, and DTS were highly consistent between pair-three latitude areas, with PSIs of SY vs. ZY (SY/ZY) above 90% (Figures 2A–C). Differently, PSIs of PH, EH, and LN for GY/ZY showed a higher discrepancy than those for SY/GY and SY/ZY (Figures 2D–F).

For the association population, PSIs of DTT, DTP, and DTS were highly consistent between pair-three latitude areas (Figure 3). In addition, PSIs of DTT, DTP, and DTS for GY/ZY and SY/GY showed lower sensitivity than those for SY/ZY (Figures 2, 3). However, PSIs of PH, EH, and LN appeared to vary inversely from those of flowering time traits. For the linkage population, PSIs of PH and LN for GY/ZY and SY/ZY showed weak sensitivity and tolerance for SY/GY; meanwhile, PSIs of EH for SY/GY, SY/ZY, and GY/ZY showed tolerance, weak sensitivity, and strong sensitivity, respectively (Figures 2D–F). The average PSIs of PH and EH for the association panel were similar between GY/ZY and SY/ZY, but PSIs of LN for SY/GY showed tolerance (Figures 3D–F). Moreover, we found that most tropic lines, such as 7031, QB2182, QB2208, S909, ZH6218, and CML171 (above 60%), have higher PSI values than temperate maize lines.

## 3.2 QTL analysis for PSI

PSIs of DTT, DTP, and DTP for $F_2$ and $F_{2:3}$ family lines showed rich variation under three different altitudes with values ranging from 20.39% (GY/ZY) to 83.87% (SY/ZY) (Table 1). The significantly positive correlations were detected between pair-PSIs of three flowering-related traits (Supplementary Table S1). The skewness and peak results were consistent with normal distribution (Figure 2), which could be used for further QTL analysis. A total of 68,994 SNP markers were used to construct the genetic linkage map, and QTL mapping is presented in Supplementary Figure S1. A total of 48 QTLs related to flowering time-related trait PSIs were identified and explained 3.67%–17.59% of phenotypic variation (PVE) (Supplementary Table S2). Among them, 17 QTLs showed PVEs of more than 10%, and 7 QTLs showed PVEs of less than 5%, indicating that PSIs for flowering time were controlled by both minor and multiple loci.

TABLE 1 The PSI analysis for QTL mapping population.

| Environments | PSI of traits | Parental lines | | F₂:₃ population lines | | |
| | | T32 | QR273 | Range | Mean ± SD | Coefficient of variation (%) |
|---|---|---|---|---|---|---|
| GY/ZY | DTT | 26.40 | 12.50 | 17.28–34.66 | 20.39 ± 5.71 | 28.00 |
| | DTP | 31.44 | 12.21 | 18.02–32.97 | 22.61 ± 5.76 | 25.46 |
| | DTS | 32.34 | 14.45 | 17.98–32.29 | 25.19 ± 6.50 | 25.80 |
| | PH | 39.08 | 27.60 | 31.17–57.82 | 52.78 ± 11.32 | 21.46 |
| | EH | 99.70 | 59.35 | 45.23–164.04 | 102.50 ± 28.74 | 28.04 |
| | LN | 57.79 | 32.77 | 32.05–81.12 | 50.79 ± 12.21 | 24.03 |
| SY/ZY | DTT | 90.68 | 58.82 | 57.02–127.88 | 83.87 ± 14.19 | 16.92 |
| | DTP | 105.65 | 59.50 | 53.79–112.06 | 80.40 ± 12.76 | 15.87 |
| | DTS | 106.20 | 59.68 | 59.09–106.50 | 83.28 ± 13.23 | 15.88 |
| | PH | 72.83 | 20.70 | 32.02–41.21 | 36.50 ± 12.01 | 32.91 |
| | EH | 122.76 | 33.64 | 48.93–72.32 | 52.89 ± 19.59 | 37.03 |
| | LN | 44.64 | 8.97 | 33.77–54.35 | 36.71 ± 10.06 | 27.41 |
| SY/GY | DTT | 50.85 | 41.18 | 33.88–69.23 | 52.64 ± 7.33 | 13.93 |
| | DTP | 56.45 | 42.15 | 30.30–59.48 | 47.06 ± 6.25 | 13.28 |
| | DTS | 55.81 | 39.52 | 34.85–56.10 | 46.37 ± 6.15 | 13.27 |
| | PH | 24.26 | −5.41 | −10.53–0.65 | −10.48 ± 6.90 | 65.82 |
| | EH | 11.55 | −16.14 | −34.74–2.55 | −23.75 ± 9.54 | 40.19 |
| | LN | −8.33 | −17.93 | −14.78–1.30 | −9.06 ± 6.40 | 70.61 |

For PSIs of DTT, six, four, and three QTLs were found for SY/GY, GY/ZY, and SY/ZY, respectively. Regarding PSIs of DTP, a total of 18 QTLs were detected between three different altitude areas, with 6, 5, and 7 QTLs to be found for SY/GY, GY/ZY, and SY/ZY, respectively. In addition, for PSIs of DTS, 2, 5, and 10 QTLs were found for SY/GY, GY/ZY, and SY/ZY, respectively. Among these QTLs, three of them exhibited pleiotropic effects: (1) both $qPSI_{DTS2}4–1$ from GY/ZY and $qPSI_{DTT3}4–1$ from SY/ZY were located at 133.4 Mb on Chr4 (Supplementary Table S2, orange blocks); (2) $qPSI_{DTP1}7–3$, $qPSI_{DTP3}7–1$, and $qPSI_{DTS3}7–3$ were positioned at 184.1 Mb on Chr7 (Supplementary Table S2, blue blocks); and (3) $qPSI_{DTP2}9–1$ and $qPSI_{DTS2}9–1$ were located at 42.5 Mb on Chr9 (Supplementary Table S2, gray blocks). It should be noted that $qPSI_{DTP1}9–1$ and $qPSI_{DTP3}9–1$ for DTP were detected for both SY/GY and SY/ZY, which were localized at 190.5 Mb on Chr9, with 13.23% and 11.98% of high PVE, respectively (Supplementary Table S2, green blocks). Both $qPSI_{DTP1}7–3$ and $qPSI_{DTP3}7–1$ were found for both SY/GY and SY/ZY, which were also positioned in the same regions (Supplementary Table S2, blue blocks).

In these QTLs, a total of 316 genes were found, including 64 candidate genes with annotated functions (Supplementary Table S3). Several important genes related to photoperiod sensitivity or flowering time-related traits were found, e.g., Zm00001d051294 at $qPSI_{DTS3}4–1$ encodes the NAC-transcription factor 27, Zm00001d012255 at $qPSI_{DTS3}2–2$ encodes the MYB-transcription factor, Zm00001d022353 at $qPSI_{DTS3}7–2$ encodes the BSD-

transcription factor 7, Zm00001d001894 at $qPSI_{DTS3}2–2$ encodes the Trihelix-transcription factor 35, Zm00001d020256 at $qPSI_{DTT2}7–1$ is the dark response gene 15, Zm00001d037749 at $qPSI_{DTS1}6–1$ encodes the bHLH-transcription factor 124, and Zm00001d017660 at $qPSI_{DTT1}5–3$ encodes Protein photoperiod-independent early flowering 1 (Supplementary Table S3). The Gene Ontology (GO) enrichment analysis indicated that 14 GO terms of most candidate genes are associated with cell, intracellular, and membrane-bounded organelle (Supplementary Figure S2A). In addition, the Kyoto Encyclopedia of Genes and Genomes (KEGG) analysis detected seven significant terms involving metabolic pathway, biosynthesis of amino acids, lysine, and monobactam (Supplementary Figure S2B).

## 3.3 GWAS for PSI

For the association population, a significantly positive correlation was also observed between PSIs of DTT, DTP, and DTS under three specific environments (Supplementary Table S4). A total of 252 significant QTNs were identified (Supplementary Table S5), with 49, 212, and 12 QTNs in GY/ZY, SY/GY, and SY/ZY, respectively (Figures 4A–C). Additionally, 43, 44, and 47 QTNs were found to be related to DTT, DTP, and DTS of PSIs for GY/ZY, in which 40 QTNs were related to all three traits (Figure 4D). Regarding PSIs for SY/GY, a total of 121, 166, and 166 QTNs were
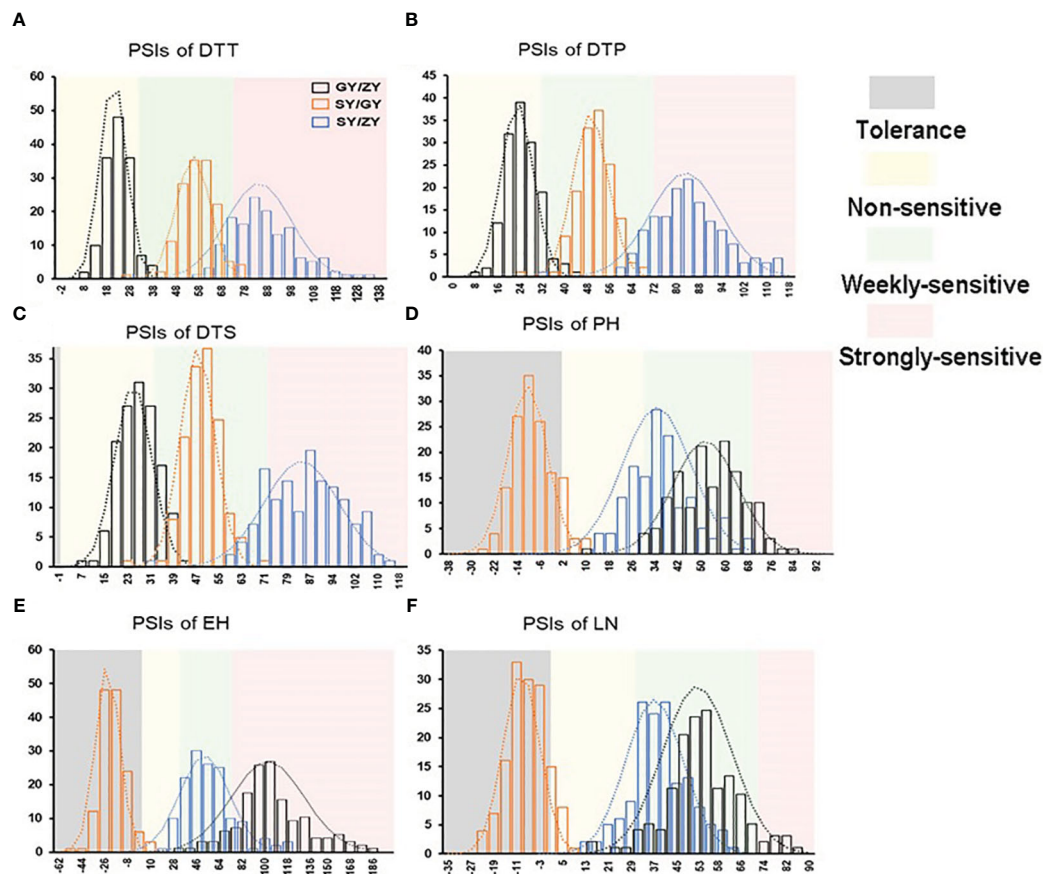
**FIGURE 2**
The histogram for PSIs of flowering time traits, **(A)** DTT, **(B)** DTP, **(C)** DTS, **(D)** PH, **(E)** EH, and **(F)** LN in the F2:3 population between pair-three latitude areas, including Guiyang vs. Zhangye (GY/ZY), Sanya vs. Guiyang (SY/GY), and Sanya vs. Zhangye (SY/ZY).

found to be associated with DTT, DTP, and DTS, respectively, wherein 78 QTNs were composed of all three traits (Figure 4E). Notably, only 12 QTNs were found to be related to PSIs for SY/ZY, wherein, 10, 10, and 8 were associated with DTT, DTP, and DTS, respectively (Figure 4F). Meanwhile, seven QTNs were found to be simultaneously related to DTT, DTP, and DTS traits (Figure 4F). These QTNs explained 9.0%–33.1% of phenotypic variation, wherein QTN of SYN1149 located on Chr5 was significantly associated with DTT, DTP, and DTS for both SY/GY and GY/ZY, which can explain 33.1% of phenotypic variation for DTT of PSI at SY/GY (Supplementary Table S5). In addition, a total of 166, 203, and 199 QTNs associated with PSI of DTT, DTP, and DTS were found, respectively (Figure 4G). Meanwhile, 117 important common QTNs were found to be related to the three traits DTT, DTP, and DTS (Figure 4G).

Among the loci mentioned above, 5,084 candidate genes were found (Supplementary Table S6), wherein 17, 55, 192, and 785 genes were found to be linked to five, four, three, and two SNPs, respectively (Supplementary Table S6). Furthermore, these candidate genes were annotated to be tRNA, lincRNA, miRNA, and transcription factors, and involved in synthetase, transferases, and binding protein function. Among these genes, *Zm00001d008700* encodes a grass-specific tryptophan aminotransferase required for vegetative and reproductive development in maize (Phillips et al., 2011), *Zm00001d021826* belongs to GRAS transcription factors that have potential roles in growth and development (Kumari et al., 2023), and *Zm00001d051012* encodes a leucine-rich repeat receptor-like protein that regulates shoot meristem proliferation in maize and determines inflorescence meristem size and yield traits in barley (Taguchi-Shiobara et al., 2001; Wang et al., 2023). In addition, the GO enrichment analysis indicated that 148 significant ($p < 0.001$) GO terms were associated with important biological processes, including transcription factor, solute antiporter, hydron symporter, and glucose transmembrane transporter activities (Supplementary Figure S3; Figure 4).

## 3.4 Transcriptome analysis

Transcriptome analysis of T32 and QR273 showed a number of differentially expressed genes (DEGs) involved in photoperiod sensitivity (Figure 5). For T32, a total of 9,343 genes were co-expressed in both SD and LD conditions, and 1,901 genes were significantly differentially expressed, including 492 genes
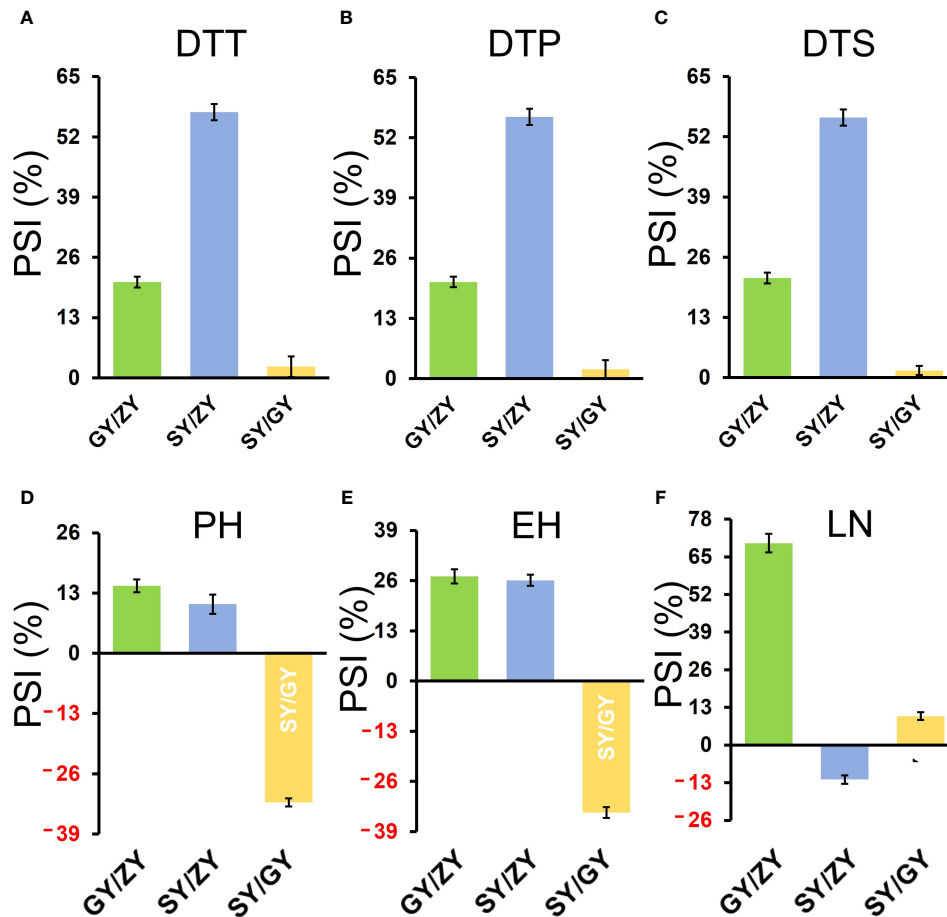
**FIGURE 3**
PSIs of DTT **(A)**, DTP **(B)**, DTS **(C)**, PH **(D)**, EH **(E)**, and LN **(F)** in the association mapping population between pair-three latitude areas, including GY/ZY, SY/GY, and SY/ZY. The Student's *t*-test was introduced for statistical analysis.
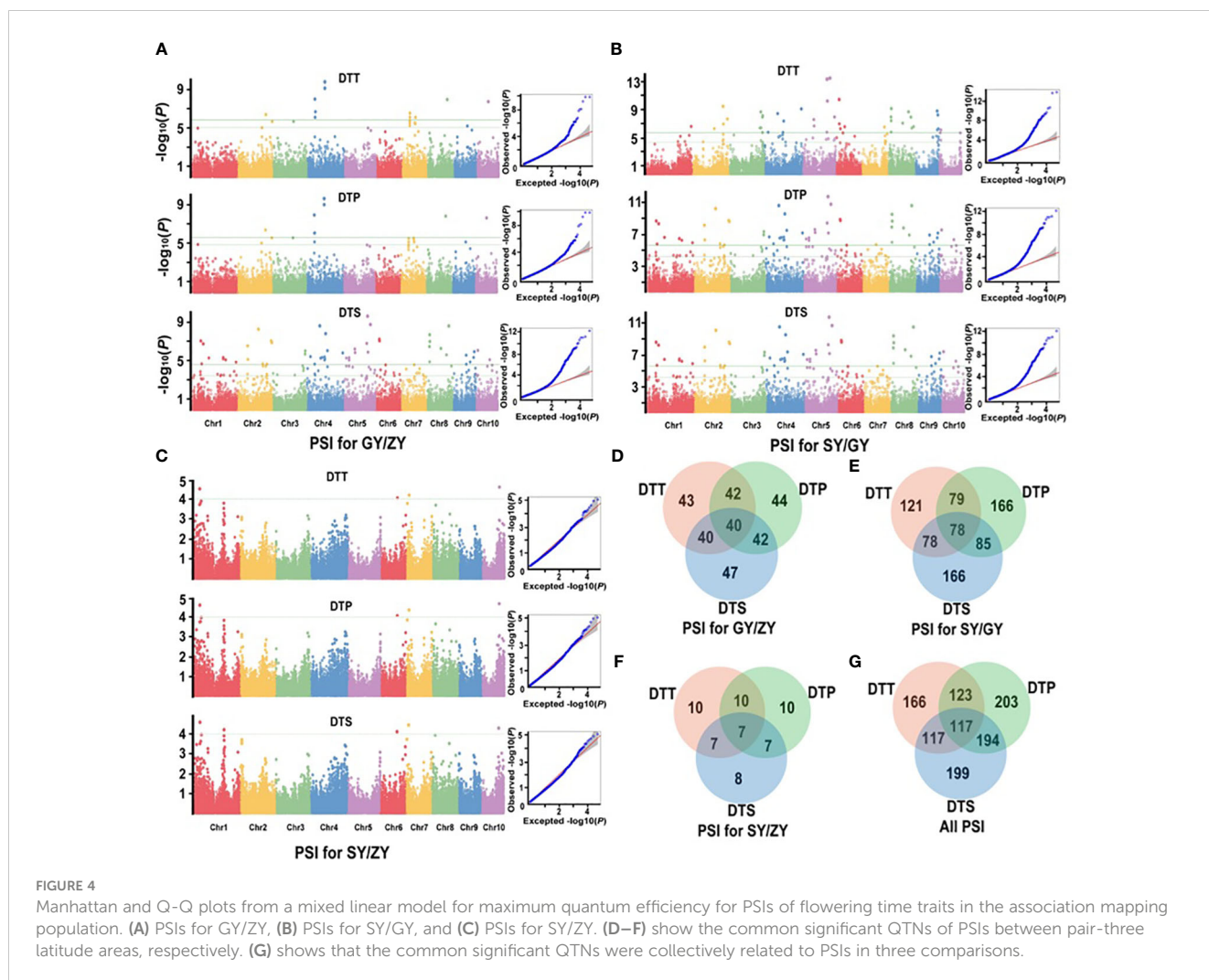
significantly upregulated and 778 genes significantly downregulated under LD conditions in comparison to those under SD conditions (Figure 5A). Meanwhile, a total of 2,963 genes were co-expressed in QR273 under both conditions, including 704 genes significantly upregulated and 916 genes significantly downregulated under LD conditions when compared to those under SD conditions (Figure 5B). Among these DEGs, 233 and 266 genes were simultaneously upregulated and downregulated for both T32 and QR273, respectively (Figure 5B).

Then, GO enrichment analyses were implemented to predict the biological processes and functions of these DEGs (Figures 5C, D). A total of 27 and 64 significant terms were detected in the upregulated and downregulated genes, respectively. Among the upregulated genes, 58, 45, and 74 genes were involved in oxidoreductase activity, biological regulation, and membrane components, respectively (Figure 5C). Regarding the downregulated genes, seven and eight genes individually participated in abscisic acid (ABA)-mediated and hormone-mediated signaling pathway, five genes were regulated by transmembrane receptor protein serine/threonine kinase activity, and nine genes were localized at the endomembrane system (Figure 5D). These results seem to imply a significant difference between the upregulated and downregulated DEGs. Furthermore, the

downregulated genes are involved in four important biological processes, namely, protein ubiquitination, ubiquitin-dependent protein catabolic process, protein amino acid autophosphorylation, and ABA-mediated signaling pathway (Supplementary Figure S5).

## 3.5 Candidate genes analysis

In this study, seven candidate genes were identified when comparing the results of linkage mapping and transcriptome analysis (Figure 6A). Here, *Zm00001d001895* and *Zm00001d034510* were downregulated for both T32 and QR273 planted under an LD environment, and these results were proven by qRT-PCR (Figure 6B). *Zm00001d001895* encodes the plant Ubiquitin Regulatory X (UBX) domain-containing protein 7 (PUX7), which functions as a negative regulator of gibberellin (GA) signaling involved in seed germination, the transition to flowering, and cell elongation and division (Hauvermale et al., 2022). *Zm00001d034510* encodes the Histidine kinase-DNA gyrase B-and HSP90-like ATPase family protein (HSP90). Its homologous genes from Arabidopsis, AtHSP90.7, have important roles in the correct folding and/or the formation of the CLV1/CLV2 transmembrane-type receptor complex that is essential

FIGURE 4

Manhattan and Q-Q plots from a mixed linear model for maximum quantum efficiency for PSIs of flowering time traits in the association mapping population. **(A)** PSIs for GY/ZY, **(B)** PSIs for SY/GY, and **(C)** PSIs for SY/ZY. **(D–F)** show the common significant QTNs of PSIs between pair-three latitude areas, respectively. **(G)** shows that the common significant QTNs were collectively related to PSIs in three comparisons.

for shoot and floral meristem development (Kadota and Shirasu, 2012). In addition, *Zm00001d034511* of T32 was upregulated when planted under LD conditions (Figure 6C), and it encodes a Golgi-localized hydroxyproline galactosyltransferase (GALT5). The homologous gene from Arabidopsis, At*GALT2*, controls AGP (arabinogalactan-proteins) O-glycosylation, which was essential for normal growth and development (Basu et al., 2015). Among the four genes of QR273, *Zm00001d034961* and *Zm00001d034514* were significantly upregulated when planted under LD conditions; in contrast, *Zm00001d046900* and *Zm00001d034515* were downregulated (Figure 6D).

Among the 5,084 genes identified by using GWAS, 203 genes were significantly and differentially expressed under LD conditions when compared to those under SD conditions. We found that 102 and 139 genes were specifically found for T32 and QR273 when planted under LD conditions. A total of 38 genes were commonly regulated for both T32 and QR273, and 15 and 23 genes were upregulated and downregulated by LD conditions in both T32 and QR273, respectively (Table 2). Notably, five genes were remarkably induced in both T32 and QR273 when plants were grown under an LD environment, namely, *Zm00001d023664*, *Zm00001d008573*, *Zm00001d021303*, *Zm00001d047664*, and *Zm00001d049244*

(Figures 7A–E). *Zm00001d023664* was involved in the hormone that could relate to plant flowering time. *Zm00001d008573* (*CaDK2C*) encoded calmodulin protein 2 and was an ortholog with Arabidopsis *AtCML23* gene (*AT1G66400*), which regulates nitric oxide levels and transition to flowering (Tsai et al., 2007; Dou et al., 2024). In addition, 36 and 66 genes from T32 were respectively upregulated and downregulated when planted under LD conditions (Figure 7F). Meanwhile, 53 and 86 genes from QR273 were remarkably upregulated and downregulated when planted under LD conditions, respectively (Figure 7F).

Four major QTLs, $qPSI_{DTP1}4–1$, $qPSI_{DTP2}3–2$, $qPSI_{DTP3}5–1$, and $qPSI_{DTP3}8–1$, were also identified by using GWAS, including 13 overlapped genes (Figure 8A), wherein *Zm00001d050238* and *Zm00001d042136* were downregulated in both T32 and QR273 planted under LD conditions (Figures 8B, C). *Zm00001d012255* and *Zm00001d008753* were upregulated in T32 but did not respond in QR273 when planted under LD conditions (Figures 8D, E); in contrast, *Zm00001d012252* was downregulated in T32 but did not respond in QR273 (Figure 8F). Interestingly, *Zm00001d008749* was downregulated in T32 but upregulated in QR273 when planted under LD conditions compared to under SD conditions (Figure 8G).
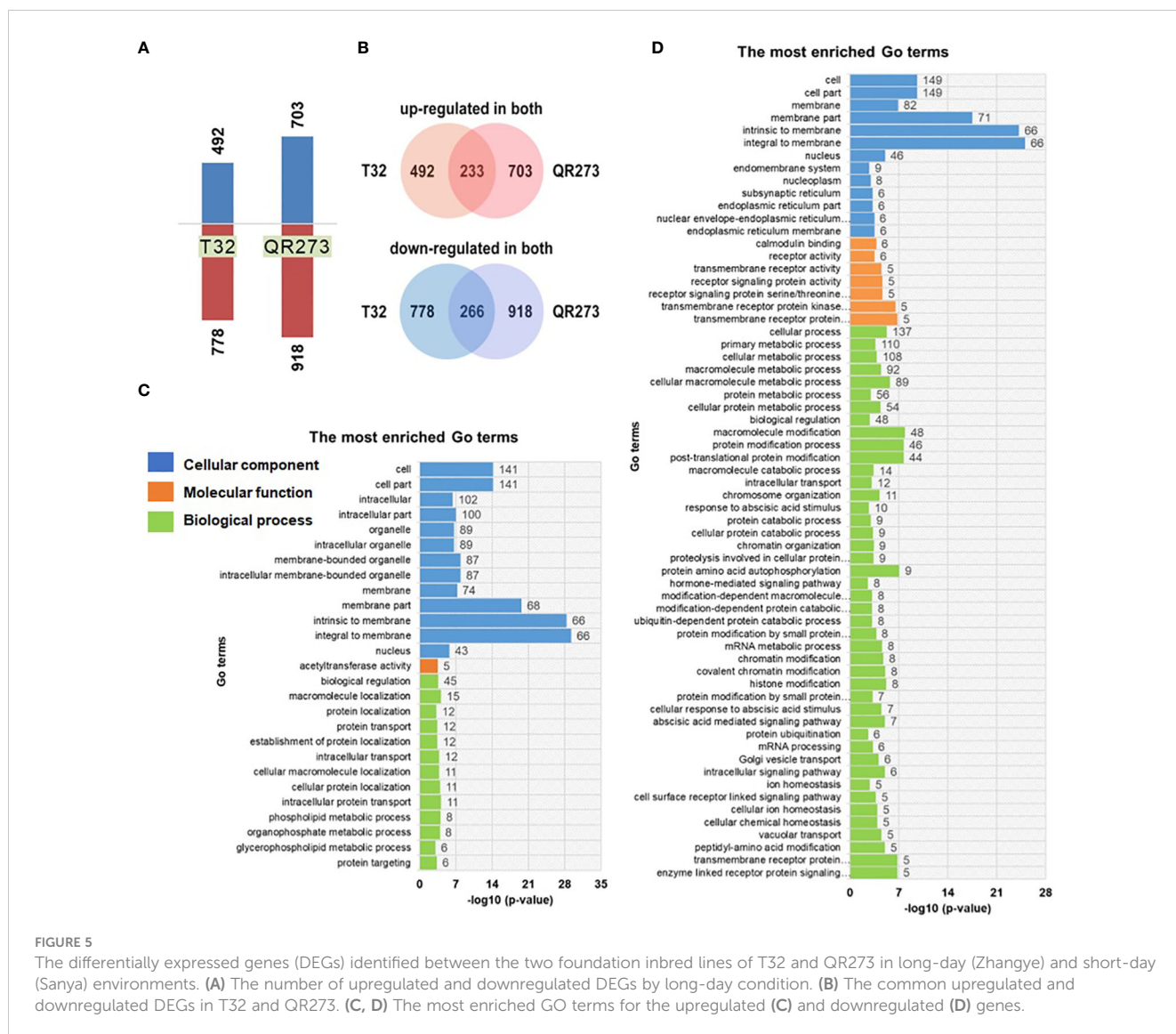
**FIGURE 5**

The differentially expressed genes (DEGs) identified between the two foundation inbred lines of T32 and QR273 in long-day (Zhangye) and short-day (Sanya) environments. **(A)** The number of upregulated and downregulated DEGs by long-day condition. **(B)** The common upregulated and downregulated DEGs in T32 and QR273. **(C, D)** The most enriched GO terms for the upregulated **(C)** and downregulated **(D)** genes.

# 4 Discussion

## 4.1 PSI is a key indicator for dissecting the genetics of maize photoperiod sensitivity

Flowering time, including DTT, DTP, and DTS, is a proper trait for PSI measurements and can be used to evaluate the photoperiod sensitivity caused by latitude discrepancy. In the current study, PSIs of DTT, DTP, and DTS analysis were highly consistent between pair-three latitude areas. However, PSIs of PH, EH, and LN showed different variants when compared to flowering time traits (Figures 2, 3). These results seemed to mean that PSIs of PH, EH, and LN did not directly reflect the influences of photoperiod. Moreover, PSIs of DTT, DTP, and DTS for GY/ZY and SY/GY were lower than those for SY/ZY (Figures 2, 3), which meant that PSI values increase with incremental latitude gap or photoperiod length. Moreover, most tropical lines, such as 7031, QB2182, QB2208, S909, ZH6218, and CML171, have higher PSI values than temperate maize lines, meaning that tropical maize basically shows more serious photoperiod sensitivity than temperate

maize. Li et al. (2020), by using 39,350 high-quality SNP markers in temperate and tropical maize groups, showed that with decreased latitude, the number of days to flowering was shortened for both temperate and tropical inbred lines, and temperate maize showed a greater difference in longer days. These results were similar to our findings.

Furthermore, QTL for the PSIs in the current results is in line with only six co-located loci in our previous study that are associated with QTL for flowering time traits (Guo et al., 2023), which meant that QTL for the PSIs is independent of the QTL for direct flowering time traits. These results were also similar to the present finding by Sabeti et al. (2002) and Li et al. (2020). Consistently, Fei et al. (2022) and Wu et al. (2023) successfully used PSI of flowering time traits to obtain significant loci and predict candidate genes. These studies mean that PSI, as an indirect trait, was also suitable for mining candidate genes, and these studies will help to understand the genetic changes during domestication and improvement and contribute to reducing the barriers to the use of tropical germplasm.
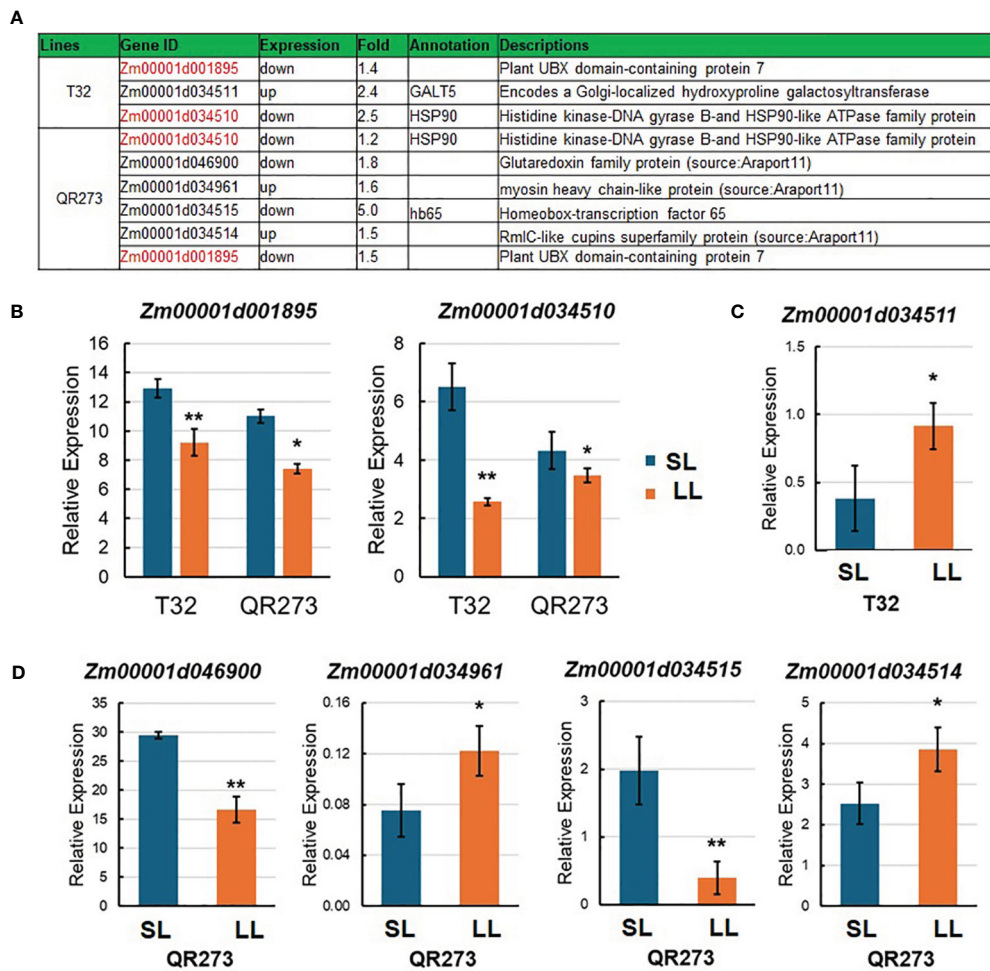
**FIGURE 6**

Information of candidate genes identified by genome-wide association study (GWAS) and transcriptome analysis. **(A)** Annotation information of seven selected candidate genes. Red text indicates DEGs in both T32 and QR273. **(B–D)** show the relative expression levels of candidate genes in T32 and/or QR273 by qRT-PCR. **(B)** The relative expression of *Zm00001d001895* and *Zm00001d034510* in both T32 and QR273, **(C)** the expression of *Zm00001d034511* in T32, and **(D)** the expression of *Zm00001d034961*, *Zm00001d034514*, *Zm00001d046900*, and *Zm00001d034515* in QR273. Asterisks (*) indicate statistically significant differences between long-day (LD) and short-day (SD) conditions (*$p < 0.05$, **$p < 0.001$).

## 4.2 PSI related genetic loci

As described above, the six QTLs in line with our previous study were $qPSI_{DTT1}9$–1, $qPSI_{DTP2}7$–1, $qPSI_{DTS2}4$–1, $qPSI_{DTP3}4$–1, $qPSI_{DTT3}4$–1, and $qPSI_{DTS3}7$–2 (Guo et al., 2023). $qPSI_{DTP3}4$–1 and $qPSI_{DTT3}4$–1 share the same region on Chr4 and are associated with two candidate genes, *Zm00001d050948* and *Zm00001d050952* (Supplementary Table S2). The two genes individually encode AP2-EREBP-transcription factor 132 (*ereb132*) and ZIM-transcription factor 49 (*zim49*), and both of them are involved in plant development, hormones, and blooming (Dietz et al., 2010; Liu et al., 2017). Furthermore, $qPSI_{DTT1}5$–2 overlapped with qPHPS1–2 associated with PSI of PH in Fei et al. (2022). In $qPSI_{DTT1}5$–2, a candidate gene, *Zm00001d016080*, was found to encode an Extra-large G-protein-like protein (XLG); is involved in maize and rice growth, development, and stress responses; and regulates agronomic traits such as PH, tiller, panicle number, heading time, and grain size/shape (Cantos et al., 2023). These results suggested that the seven QTLs may be hotspot regions related to maize photoperiod

sensitivity. Among the total 64 annotated genes detected in this paper, 3 known flowering time-related genes, *ZCN4* (*Zm00001d003804*) belonging to FLOWERING LOCUS T (FT) members, *BURP8* (*Zm00001d050241*), and *AVT1I* (*Zm00001d037229*), can regulate maize flowering (Azodi et al., 2019; Su et al., 2024). *Zm00001d017660* is annotated as protein photoperiod-independent early flowering 1.

## 4.3 QTNs related to PSI

In maize, several studies were conducted to identify QTNs and candidate genes involved in photoperiod sensitivity through GWAS analysis. Yang et al. (2013) performed a GWAS using 368 inbred lines of maize and identified 48 polymorphic sites associated with flowering time, in which 42 of the 48 sites were located within the promoter region of the *ZmCCT* gene that was an important gene that attenuated photoperiod sensitivity. Li et al. (2020) revealed 106 selective-sweep regions containing 423 candidate genes using

TABLE 2 Annotation information of 38 selected candidate genes by GWAS and transcriptome data.

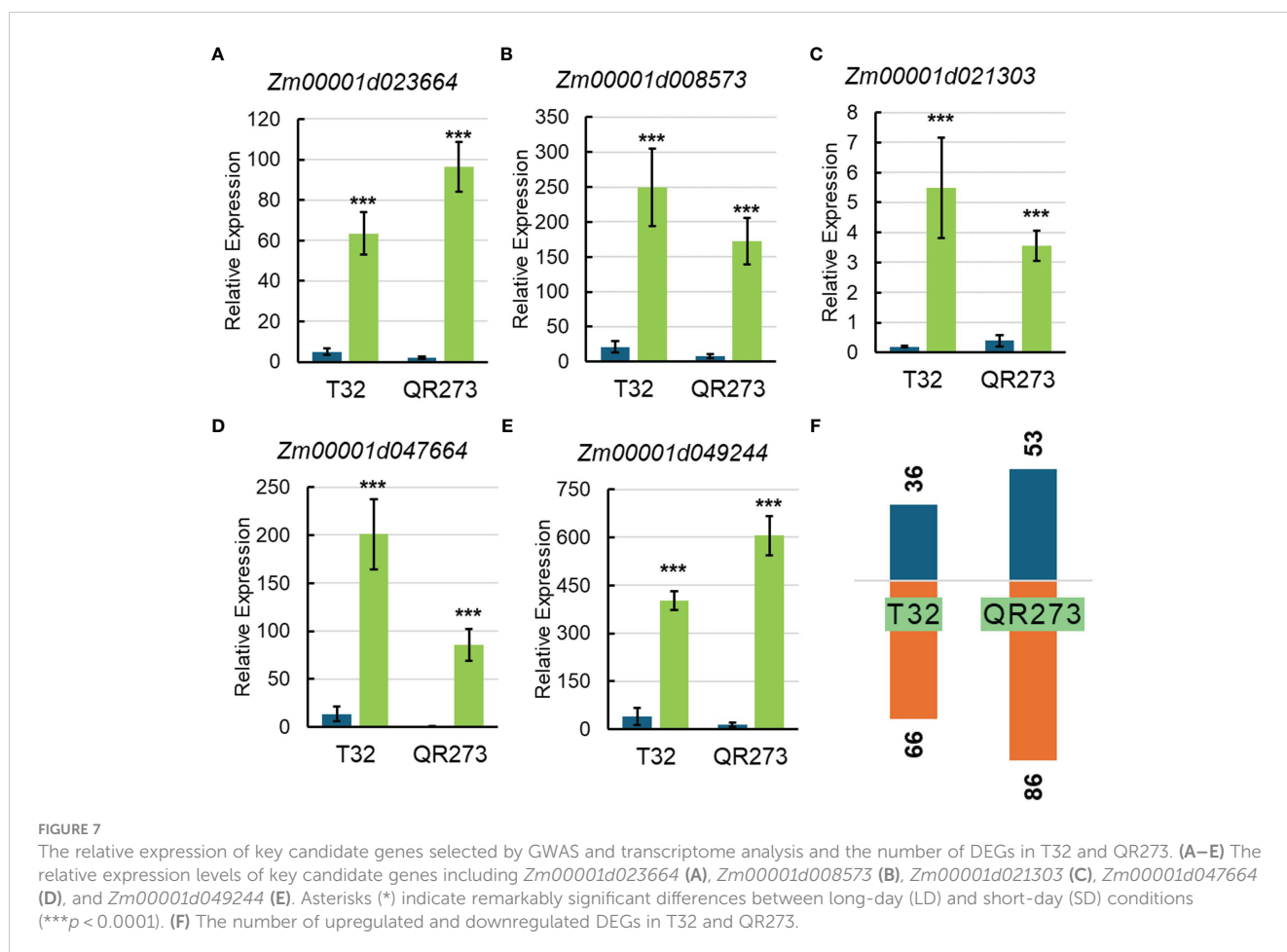| Genes | Expression | Fold | Expression | Fold | Annotation | Description |
|---|---|---|---|---|---|---|
| | T32 | | QR273 | | | |
| Zm00001d035481 | Down | 1.62 | Down | 2.70 | MYND | Programmed cell death protein 2 C-terminal domain-containing protein |
| Zm00001d006030 | Down | 1.29 | Down | 1.34 | ENT | ENT domain containing protein |
| Zm00001d033860 | Down | 2.08 | Down | 2.58 | | Uncharacterized |
| Zm00001d034370 | Down | 2.43 | Down | 3.29 | | F-type ATPase gamma/ML domain protein |
| Zm00001d007214 | Down | 1.61 | Down | 1.15 | TIM44–2 | Mitochondrial import inner membrane translocase subunit TIM44–2 |
| Zm00001d003904 | Down | 2.13 | Down | 1.52 | TRAPP | Transport protein particle (TRAPP) component |
| Zm00001d008708 | Down | 2.08 | Down | 1.94 | DUF | Putative DUF1421 domain family protein |
| Zm00001d008743 | Down | 1.93 | Down | 1.23 | | Ubiquitin carboxyl-terminal hydrolase |
| Zm00001d008748 | Down | 2.50 | Down | 2.21 | | Uncharacterized |
| Zm00001d011927 | Down | 3.34 | Down | 5.88 | | Uncharacterized |
| Zm00001d012307 | Down | 5.67 | Down | 1.96 | nbcs22 | Nucleobase: cation symporter 22 |
| Zm00001d013336 | Down | 1.53 | Down | 1.52 | BED | Zinc finger BED domain-containing protein DAYSLEEPER |
| Zm00001d013712 | Down | 2.28 | Down | 1.92 | FLK | Flowering locus K homology domain |
| Zm00001d021595 | Down | 1.91 | Down | 1.27 | | Uncharacterized |
| Zm00001d027503 | Down | 2.07 | Down | 2.20 | CBEF | Calcium-binding EF hand family protein |
| Zm00001d036055 | Down | 2.91 | Down | 2.13 | | Uncharacterized |
| Zm00001d037058 | Down | 1.45 | Down | 1.57 | CAK1AT | Encodes a CDK-activating kinase that regulates root initial cell differentiation |
| Zm00001d037604 | Down | 2.30 | Down | 2.99 | ETR3 | Ethylene receptor homolog 3 |
| Zm00001d037606 | Down | 2.03 | Down | 2.14 | imp2/ ARM42/IMPa3 | Importin 2/Importin subunit alpha |
| Zm00001d039341 | Down | 3.34 | Down | 2.14 | EIN2 | Ethylene insensitive 2 |
| Zm00001d044188 | Down | 2.34 | Down | 1.51 | | Glycosyl transferase family 1 protein |
| Zm00001d048224 | Down | 2.19 | Down | 2.62 | VQ57 | VQ motif-transcription factor 57 |
| Zm00001d053701 | Down | 6.60 | Down | 6.53 | | Nuclear pore complex protein NUP 96 |
| Zm00001d028948 | Up | 2.47 | Up | 4.63 | cal3 | Calmodulin 3 |
| Zm00001d028941 | Up | 10.99 | Up | 4.35 | vp3 | VQ motif-transcription factor 3 |
| Zm00001d034372 | Up | 3.39 | Up | 5.47 | cdpk50/cpk11 | Calcium-dependent protein kinase 50 |
| Zm00001d023664 | Up | 12.62 | Up | 49.04 | | ABA-responsive protein |
| Zm00001d008573 | Up | 11.68 | Up | 20.94 | CaDK2C | Calmodulin protein 2, touch-induced |
| Zm00001d044033 | Up | 2.95 | Up | 2.50 | YLS7 | Trichome birefringence-like 20/tbl17, yellow-leaf-specific gene 7 |
| Zm00001d011256 | Up | 2.02 | Up | 1.50 | ohp3 | Opaque 2 heterodimerizing protein 3 |
| Zm00001d013333 | Up | 3.32 | Up | 12.51 | | Uncharacterized |
| Zm00001d016591 | Up | 1.65 | Up | 1.93 | | Serine/threonine-protein kinase PBS1; probable serine/threonine-protein kinase PBL7 |

*(Continued)*

TABLE 2 Continued

| Genes | Expression | Fold | Expression | Fold | Annotation | Description |
|---|---|---|---|---|---|---|
| | T32 | | QR273 | | | |
| Zm00001d020100 | Up | 2.56 | Up | 3.83 | prh6/PP2C-A4 | Protein phosphatase homolog 6 |
| Zm00001d021303 | Up | 28.15 | Up | 9.12 | | Uncharacterized |
| Zm00001d031807 | Up | 6.79 | Up | 5.68 | | Solute carrier family 25 member 44 |
| Zm00001d046471 | Up | 7.26 | Up | 16.50 | mbf2 | Multi-protein bridging factor homolog 2 |
| Zm00001d047664 | Up | 14.85 | Up | 97.67 | | Uncharacterized |
| Zm00001d049244 | Up | 9.90 | Up | 40.99 | BAG | BAG domain-containing protein |

39,350 high-quality SNP markers in temperate and tropical maize groups consisting of 410 inbred lines phenotyping in three representative experiments in different latitudes.

In this study, a total of 252 SNPs and 5,084 genes within a 1-Mb region (Li et al., 2016a) for PSI of the flowering time traits were found in maize planting in different latitude areas. Compared to our previous studies, one (PZE-102181889) and four (PZE-108077370, SYN4993, SYN34850, and PZE-109065940) common SNPs were found in Wu et al. (2023) and Li et al. (2016b), respectively. Among these candidate genes associated with the above SNPs,

Zm00001d007191 belongs to the MYB-transcription family this family has proven functions for plant flowering (Liu et al., 2014; Zhu et al., 2020; Hong et al., 2021; Wu et al., 2023). *Zm00001d007188*, belonging to Ethylene-insensitive 3 (EIN3)/ EIN3-Like (EIL) transcription factors, is a core component of the ethylene signaling pathway that plays important roles in plant development and flowering (Mao et al., 2022). *Zm00001d023592*, *Zm00001d023593*, and *Zm00001d023596* encode the amino acid/ auxin permease 64, 65, and 66 (*aaap64/65/66*), respectively. Their homology *AAP2/3/5* from Arabidopsis participated in the high-
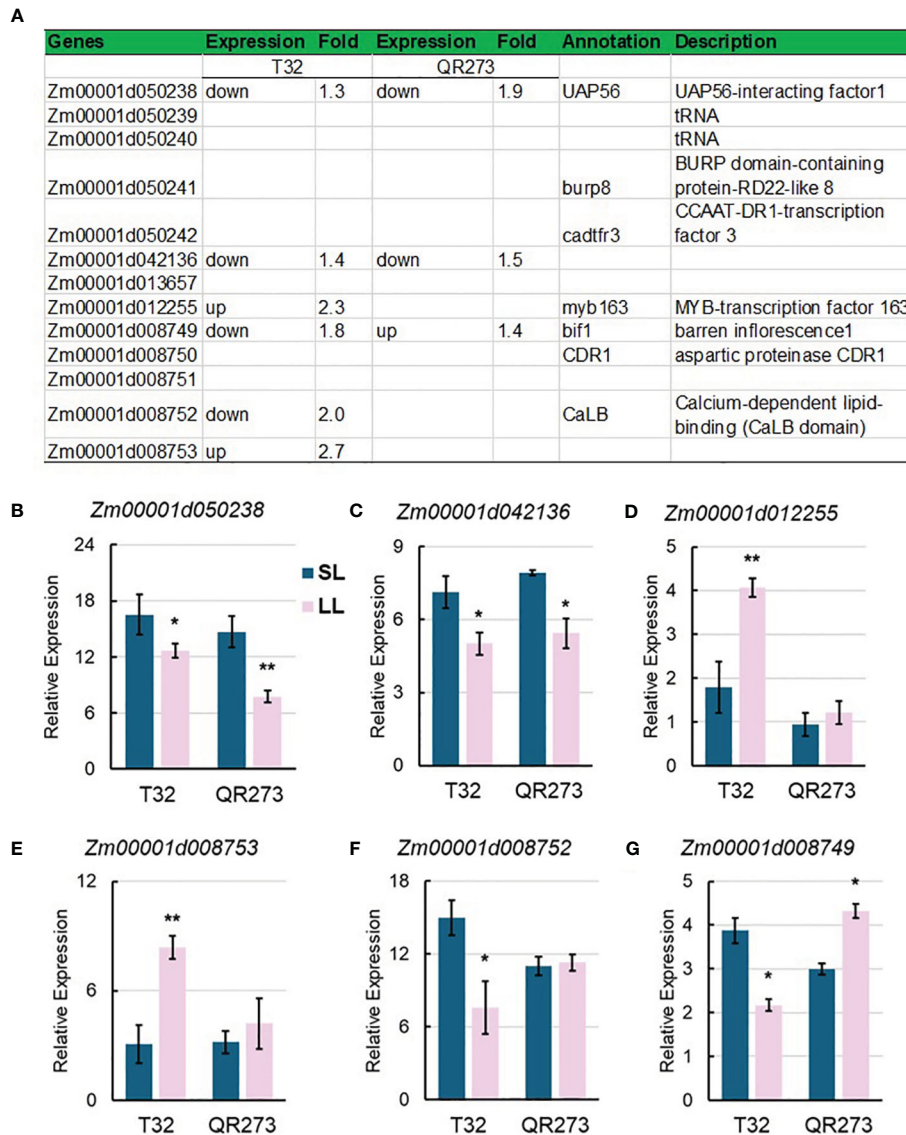


FIGURE 7
The relative expression of key candidate genes selected by GWAS and transcriptome analysis and the number of DEGs in T32 and QR273. **(A−E)** The relative expression levels of key candidate genes including *Zm00001d023664* **(A)**, *Zm00001d008573* **(B)**, *Zm00001d021303* **(C)**, *Zm00001d047664* **(D)**, and *Zm00001d049244* **(E)**. Asterisks (*) indicate remarkably significant differences between long-day (LD) and short-day (SD) conditions (***$p < 0.0001$). **(F)** The number of upregulated and downregulated DEGs in T32 and QR273.

**FIGURE 8**

Information of candidate genes identified by QTL and GWAS analysis. **(A)** Annotation information of 13 selected candidate genes. **(B–D)** show the relative expression levels of main candidate genes by qRT-PCR including *Zm00001d050238* **(B)**, *Zm00001d042136* **(C)**, *Zm00001d012255* **(D)**, *Zm00001d008753* **(E)**, *Zm00001d012252* **(F)**, and *Zm00001d008749* **(G)**. Asterisks (*) indicate statistically significant differences between long-day (LL) and short-day (SL) conditions (*$p < 0.05$, **$p < 0.001$).

affinity transport system for acidic and neutral amino acids in the tapetum cells of Arabidopsis flowers (Lee and Tegeder, 2004). Interestingly, a small auxin-up RNA gene (*SAUR*) cluster was in the region of SYN34850, including *SAUR65, 66, 67*, and *68*, and many previous studies have shown that *SAUR* genes play important roles in heading date, flower morphogenesis, and pollination by inducing auxin (Kant et al., 2009; Ke et al., 2018; Sun et al., 2023). For example, *SAUR63* promotes hypocotyl and stamen filament elongation in Arabidopsis (Chae et al., 2012); *SAUR62/75* are required for the translation of transcripts essential for pollen tube growth (He et al., 2018); *SAUR7* possibly regulates the development of flower organs in apples (Wang et al., 2020); *SAUR56* regulates heading date in rice (Zhao et al., 2023).

## 4.4 Common genetic loci related to PSI via combined analysis

The joint analysis of combining multiple methods, such as the GWAS approach, linkage analysis, and transcriptome analysis, to quickly find key candidate genes has proven to be effective. Hung et al. (2012) found 25 candidate genes, including important and known flowering genes *IF-4A*, *Id1*, and *Vgt1*, mapped within both joint linkage QTL and GWAS of photoperiod sensitivity for thermal time to silking in maize NAM and IBM populations. Similarly, Li et al. (2021) identified the *WRKY14* gene by combining GWAS and linkage analysis, which is a critical regulator of maize flowering time and LN. In this study, 13 overlapped genes were found by integrating

the results of GWASs, QTL mapping, and transcriptome analysis, and five putative key candidate genes (*MYB163*, *BIF1*, *BURP8*, *CADR3*, and *Zm00001d050238*) were selected.

In detail, *Zm00001d012255* encodes MYB-transcription factor 163, and MYB proteins are key factors in regulatory networks controlling the development, metabolism, and responses to biotic and abiotic stresses (Dubos et al., 2010). For example, *PtrMYB192*, a *Populus* R2R3 MYB transcription factor, regulates flowering time in Arabidopsis by activating FLOWERING LOCUS C (Liu et al., 2013). The overexpression of an apple R2R3 MYB transcription factor, *MdMYB3*, has resulted in transcriptional activation of several flavonoid pathway genes and produced longer peduncles and pistil styles of flowers than those of wild-type plants, meaning that it is involved in the regulation of flower development (Vimolmangkang et al., 2013). *Zm00001d008749* was remarked to be associated with the mutant *bif1* that causes barren inflorescence. Previous research found that two BIF genes, BIF1 and BIF4, encode AUXIN/INDOLE-3-ACETIC ACID (Aux/IAA) proteins and regulate the early steps required for inflorescence formation by the auxin hormone signaling pathway (Galli et al., 2015). Notably, *Zm00001d050238* was reported to be involved in the *cis*-regulation underlying maize highland adaptation that is also highly related to traits like maize flowering time (Hu et al., 2022).

In addition, the two genes *Zm00001d050241* and *Zm00001d050242* may be indirectly related to maize flowering. *Zm00001d050241* encodes BURP domain-containing protein-RD22-like 8 (*BURP8*), in which BURP genes are differentially responsive to ABA and ABA-related stress conditions (Matus et al., 2014). *ZmBURP8* participates in the ABA-responsive pathway by *ZmPRR37* regulation, in which ZmPRR37-CR knockout mutants exhibited early flowering compared to WT under LD conditions (Su et al., 2024). *Zm00001d050242* encodes CCAAT-DR1-transcription factor 3 (CADR3) and belongs to the NUCLEAR FACTOR-Y (NF-Y) family; NF-Ys have been shown to play an important role in growth, development, and the response to environmental stress (Zhang et al., 2016). Those potential candidate genes via joint analysis would greatly advance our understanding of maize photoperiod sensitivity.

## 4.5 Conclusion

In conclusion, PSIs of DTT, DTP, and DTS showed efficacious interactions with photoperiod sensitivity for maize latitude adaptation. Based on the analysis of PSIs in the study, a total of 48 QTLs and 252 significant SNPs were identified by linkage mapping and the GWAS approach, respectively. Five critical candidate genes, *MYB163*, *BIF1*, *BURP8*, *CADR3*, and *Zm00001d050238*, were significantly associated with photoperiod sensitivity, which could be deeply studied in further research. These results may provide much more abundant theoretical proof to reveal the genetic basis of photoperiod sensitivity, which would be beneficial for tropical germplasm improvement in current maize molecular design-based breeding.

## Data availability statement

The original contributions presented in the study are included in the article/Supplementary Material, further inquiries can be directed to the corresponding author/s.

## Author contributions

YJ: Writing – review & editing, Writing – original draft, Validation, Formal analysis, Conceptualization. SG: Data curation, Formal analysis, Software, Writing – review & editing. DW: Data curation, Formal analysis, Software, Writing – review & editing. LT: Writing – original draft, Software, Formal analysis, Data curation. PL: Writing – original draft, Software, Formal analysis, Data curation. XG: Writing – original draft, Software, Formal analysis, Data curation. AW: Writing – review & editing, Data curation. YZ: Writing – review & editing, Data curation. XL: Writing – review & editing, Data curation. ZC: Writing – review & editing, Supervision, Project administration, Methodology, Funding acquisition. XW: Writing – review & editing, Methodology, Conceptualization.

## Funding

## Conflict of interest

The authors declare that the research was conducted in the absence of any commercial or financial relationships that could be construed as a potential conflict of interest.

## Publisher's note

All claims expressed in this article are solely those of the authors and do not necessarily represent those of their affiliated organizations, or those of the publisher, the editors and the reviewers. Any product that may be evaluated in this article, or

claim that may be made by its manufacturer, is not guaranteed or endorsed by the publisher.

## Supplementary material

The Supplementary Material for this article can be found online at: https://www.frontiersin.org/articles/10.3389/fpls.2024.1441288/full#supplementary-material

## References

Azodi, C. B., Pardo, J., VanBuren, R., de Los Campos, G., and Shiu, S. H. (2019). Transcriptome-based prediction of complex traits in maize. *Plant Cell* 32, 139–151. doi: 10.1105/tpc.19.00332

Basu, D., Wang, W., Ma, S., DeBrosse, T., Poirier, E., Emch, K., et al. (2015). Two hydroxyproline galactosyltransferases, GALT5 and GALT2, function in arabinogalactan-protein glycosylation, growth and development in Arabidopsis. *PloS One* 10, e0125624. doi: 10.1371/journal.pone.0125624

Birch, C. J., Hammer, G. L., and Rickert, K. G. (1998). Temperature and photoperiod sensitivity of development in five cultivars of maize (*Zea mays* L.) from emergence to tassel initiation. *Field Crops Res.* 55, 93–107. doi: 10.1016/S0378-4290(97)00062-2

Cantos, C. F., Depamphilis, C. W., and Assmann, S. M. (2023). Extra-large G proteins have extra-large effects on agronomic traits and stress tolerance in maize and rice. *Trends Plant Sci.* 28, 1033–1044. doi: 10.1016/j.tplants.2023.04.005

Chae, K., Isaacs, C. G., Reeves, P. H., Maloney, G. S., Muday, G. K., Nagpal, P., et al. (2012). Arabidopsis SMALL AUXIN UP RNA63 promotes hypocotyl and stamen filament elongation. *Plant J.* 71, 684–697. doi: 10.1111/j.1365-313X.2012.05024.x

Colasanti, J., and Muszynski, M. (2009). "The maize floral transition," in *Handbook of maize: its biology*, 41–55.

Dietz, K. J., Vogel, M. O., and Viehhauser, A. (2010). AP2/EREBP transcription factors are part of gene regulatory networks and integrate metabolic, hormonal and environmental signals in stress acclimation and retrograde signaling. *Protoplasma* 245, 3–14. doi: 10.1007/s00709-010-0142-8

Dou, D., Sun, J., Abou-Elwafa, S. F., Guo, X., Guo, Y., Wang, D., et al. (2024). *ZmILI1* confers salt stress tolerance by regulating genes of phytohormone response in maize. *Environ. Exp. Bot.* 224, 105673. doi: 10.1016/j.envexpbot.2024.105673

Du, F., Tao, Y., Ma, C., Zhu, M., Guo, C., and Xu, M. (2023). Effects of the quantitative trait locus qPss3 on inhibition of photoperiod sensitivity and resistance to stalk rot disease in maize. *Theor. Appl. Genet.* 136, 126. doi: 10.1007/s00122-023-04370-6

Dubos, C., Stracke, R., Grotewold, E., Weisshaar, B., Martin, C., and Lepiniec, L. (2010). MYB transcription factors in Arabidopsis. *Trends Plant Sci.* 15, 573–581. doi: 10.1016/j.tplants.2010.06.005

Edmeades, G. O., Trevisan, W., Prasanna, B. M., and Campos, H. (2017). Tropical maize (*Zea mays* L.). *Genet. improve. Trop. Crops*, 57–109. doi: 10.1007/978-3-319-59819-2_3

Fei, J., Jiang, Q., Guo, M., Lu, J., Wang, P., Liu, S., et al. (2022). Fine mapping and functional research of key genes for photoperiod sensitivity in maize. *Front. Plant Sci.* 13, 890780. doi: 10.3389/fpls.2022.890780

Galli, M., Liu, Q., Moss, B. L., Malcomber, S., Li, W., Gaines, C., et al. (2015). Auxin signaling modules regulate maize inflorescence architecture. *PNAS* 112, 13372–13377. doi: 10.1073/pnas.1516473112

Gehrig, H. H., Winter, K., Cushman, J., Borland, A., and Taybi, T. (2000). An improved RNA isolation method for succulent plant species rich in polyphenols and polysaccharides. *Plant Mol. Biol. Rep.* 18, 369–376. doi: 10.1007/BF02825065

Guo, S., Wang, D., Niu, L., He, Y., Tu, L., Liu, P., et al. (2023). QTL mapping and candidate gene analysis of maize flower time related traits. *Seed* 42, 108. doi: 10.1186/s12870-022-03711-9

Hauvermale, A. L., Cárdenas, J. J., Bednarek, S. Y., and Steber, C. M. (2022). GA signaling expands: the plant UBX domain-containing protein 1 is a binding partner for the GA receptor. *Plant Physiol.* 190, 2651–2670. doi: 10.1093/plphys/kiac406

He, S. L., Hsieh, H. L., and Jauh, G. Y. (2018). SMALL AUXIN UP RNA62/75 are required for the translation of transcripts essential for pollen tube growth. *Plant Physiol.* 178, 626–640. doi: 10.1104/pp.18.00257

Hong, L., Niu, F., Lin, Y., Wang, S., Chen, L., and Jiang, L. (2021). MYB106 is a negative regulator and a substrate for CRL3BPM E3 ligase in regulating flowering time in Arabidopsis thaliana. *J. Integr. Plant Biol.* 63, 1104–1119. doi: 10.1111/jipb.13071

Hu, H., Crow, T., Nojoomi, S., Schulz, A. J., Estévez-Palmas, J. M., Hufford, M. B., et al. (2022). Allele-specific expression reveals multiple paths to highland adaptation in maize. *Mol. Biol. Evol.* 39, 239. doi: 10.1093/molbev/msac239

Hung, H. Y., Shannon, L. M., Tian, F., Bradbury, P. J., Chen, C., Flint-Garcia, S. A., et al. (2012). *ZmCCT* and the genetic basis of day-length adaptation underlying the postdomestication spread of maize. *PNAS* 109, E1913–E1921. doi: 10.1073/pnas.1203189109

Jiang, Y., Chen, X., Chai, S., Sheng, H., Sha, L., Fan, X., et al. (2021). TpIRT1 from Polish wheat (*Triticum polonicum* L.) enhances the accumulation of Fe, Mn, Co, and Cd in Arabidopsis. *Plant Sci.* 312, 111058. doi: 10.1016/j.plantsci.2021.111058

Kadota, Y., and Shirasu, K. (2012). The HSP90 complex of plants. *Biochim. Biophys. Acta (BBA)-Mol. Cell Res.* 1823, 689–697. doi: 10.1016/j.bbamcr.2011.09.016

Kant, S., Bi, Y. M., Zhu, T., and Rothstein, S. J. (2009). SAUR39, a small auxin-up RNA gene, acts as a negative regulator of auxin synthesis and transport in rice. *Plant Physiol.* 151, 691–701. doi: 10.1104/pp.109.143875

Ke, M., Gao, Z., Chen, J., Qiu, Y., Zhang, L., and Chen, X. (2018). Auxin controls circadian flower opening and closure in the waterlily. *BMC Plant bio.* 18, 1–21. doi: 10.1186/s12870-018-1357-7

Khotasena, S., Sanitchon, J., Chankaew, S., and Monkham, T. (2022). The basic vegetative phase and Photoperiod Sensitivity Index as the major criteria for indigenous upland rice production in Thailand under unpredictable conditions. *Agronomy* 12, 957. doi: 10.3390/agronomy12040957

Kumari, P., Gahlaut, V., Kaur, E., Singh, S., Kumar, S., and Jaiswal, V. (2023). Genome-wide identification of GRAS transcription factors and their potential roles in growth and development of roses (*Rosa chinensis*). *J. Plant Growth Regul.* 42, 1505–1521. doi: 10.1007/s00344-022-10635-z

Langdale, J. (2005). The then and now of maize leaf development. *Maydica* 50 (3–4), 459–467.

Lee, Y. H., and Tegeder, M. (2004). Selective expression of a novel high-affinity transport system for acidic and neutral amino acids in the tapetum cells of Arabidopsis flowers. *Plant J.* 40, 60–74. doi: 10.1111/j.1365-313X.2004.02186.x

Li, Y. X., Li, C., Bradbury, P. J., Liu, X., Lu, F., Romay, C. M., et al. (2016b). Identification of genetic variants associated with maize flowering time using an extremely large multi-genetic background population. *Plant J.* 86, 391–402. doi: 10.1111/tpj.13174

Li, Z., Li, K., Yang, X., Hao, H., and Jing, H. C. (2021). Combined QTL mapping and association study reveals candidate genes for leaf number and flowering time in maize. *Theor. Appl. Genet.* 134, 3459–3472. doi: 10.1007/s00122-021-03907-x

Li, Z., Liu, X., Xu, X., Liu, J., Sang, Z., Yu, K., et al. (2020). Favorable haplotypes and associated genes for flowering time and photoperiod sensitivity identified by comparative selective signature analysis and GWAS in temperate and tropical maize. *Crop J.* 8, 227–242. doi: 10.1016/j.cj.2019.09.012

Li, D., Wang, X., Zhang, X., Chen, Q., Xu, G., Xu, D., et al. (2016a). The genetic architecture of leaf numbers and its genetic relationship to flowering time in maize. *New Phyt.* 210, 256–268. doi: 10.1111/nph.13765

Liu, F., Sun, T., Wang, L., Su, W., Gao, S., Su, Y., et al. (2017). Plant jasmonate ZIM domain genes: shedding light on structure and expression patterns of JAZ gene family in sugarcane. *BMC Gen.* 18, 1–17. doi: 10.1186/s12864-017-4142-3

Liu, S., Wang, X., Li, E., Douglas, C. J., Chen, J. G., and Wang, S. (2013). R2R3 MYB transcription factor PtrMYB192 regulates flowering time in Arabidopsis by activating FLOWERING LOCUS C. *J. Plant Bio.* 56, 243–250. doi: 10.1007/s12374-013-0135-1

Liu, L., Zhang, J., Adrian, J., Gissot, L., Coupland, G., Yu, D., et al. (2014). Elevated levels of MYB30 in the phloem accelerate flowering in Arabidopsis through the regulation of FLOWERING LOCUS T. *PloS One* 9, e89799. doi: 10.1371/journal.pone.0089799

Mao, K., Zhang, M., Kong, Y., Wang, Y., Meng, Q., Ma, N., et al. (2022). Origin, expansion, and divergence of ETHYLENE-INSENSITIVE 3 (EIN3)/EIN3-LIKE transcription factors during streptophytes evolution. *Front. Plant Sci.* 13, 858477. doi: 10.3389/fpls.2022.858477

Matus, J. T., Aquea, F., Espinoza, C., Vega, A., Cavallini, E., Santo, S. D., et al. (2014). Inspection of the grapevine BURP superfamily highlights an expansion of RD22 genes with distinctive expression features in berry development and ABA-mediated stress responses. *PloS One* 9, e110372. doi: 10.1371/journal.pone.0110372

Phillips, K. A., Skirpan, A. L., Liu, X., Christensen, A., Slewinski, T. L., Hudson, C., et al. (2011). Vanishing tassel2 encodes a grass-specific tryptophan aminotransferase required for vegetative and reproductive development in maize. *Plant Cell* 23, 550–566. doi: 10.1105/tpc.110.075267

Sabeti, P. C., Reich, D. E., Higgins, J. M., Levine, H. Z., Richter, D. J., Schaffner, S. F., et al. (2002). Detecting recent positive selection in the human genome from haplotype structure. *Nature* 419, 832–837. doi: 10.1038/nature01140

Saghai-Maroof, M. A., Soliman, K. M., Jorgensen, R. A., and Allard, R. (1984). Ribosomal DNA spacer-length polymorphisms in barley: mendelian inheritance, chromosomal location, and population dynamics. *PNAS* 81, 8014–8018. doi: 10.1073/pnas.81.24.8014

Su, H., Cao, L., Ren, Z., Sun, W., Zhu, B., Ma, S., et al. (2024). ZmELF6-ZmPRR37 module regulates maize flowering and salt response. *Plant Bio. J.* 22, 929–945. doi: 10.1111/pbi.14236

Sun, J., Zheng, Y., Guo, J., Zhang, Y., Liu, Y., Tao, Y., et al. (2023). GmGAMYB-BINDING PROTEIN 1 promotes small auxin-up RNA gene transcription to modulate soybean maturity and height. *Plant Physiol.* 193, 775–791. doi: 10.1093/plphys/kiad293

Taguchi-Shiobara, F., Yuan, Z., Hake, S., and Jackson, D. (2001). The fasciated ear2 gene encodes a leucine-rich repeat receptor-like protein that regulates shoot meristem proliferation in maize. *Genes Dev.* 15, 2755–2766. doi: 10.1101/gad.208501

Tsai, Y. C., Delk, N. A., Chowdhury, N. I., and Braam, J. (2007). Arabidopsis potential calcium sensors regulate nitric oxide levels and the transition to flowering. *Plant Signal. Behav.* 2, 446–454. doi: 10.4161/psb.2.6.4695

Vimolmangkang, S., Han, Y., Wei, G., and Korban, S. S. (2013). An apple MYB transcription factor, MdMYB3, is involved in regulation of anthocyanin biosynthesis and flower development. *BMC Plant bio.* 13, 1–13. doi: 10.1186/1471-2229-13-176

Wang, P., Gong, R., Yang, Y., and Yu, S. (2019). *Ghd8* controls rice photoperiod sensitivity by forming a complex that interacts with Ghd7. *BMC Plant bio.* 19, 1–14. doi: 10.1186/s12870-019-2053-y

Wang, P., Lu, S., Xie, M., Wu, M., Ding, S., Khaliq, A., et al. (2020). Identification and expression analysis of the small auxin-up RNA (SAUR) gene family in apple by inducing of auxin. *Gene* 750, 144725. doi: 10.1016/j.gene.2020.144725

Wang, C., Yang, X., Zhang, Y., Shen, C., Shi, J., Xia, C., et al. (2023). Barley FASCIATED EAR genes determine inflorescence meristem size and yield traits. *Crop J.* 11, 679–691. doi: 10.1016/j.cj.2022.10.001

Wu, X., Liu, Y., Lu, X., Tu, L., Gao, Y., Wang, D., et al. (2023). Integration of GWAS, linkage analysis and transcriptome analysis to reveal the genetic basis of flowering time-related traits in maize. *Front. Plant Sci.* 14, 1145327. doi: 10.3389/fpls.2023.1145327

Wu, X., Wang, A., Guo, X., Liu, P., Zhu, Y., Li, X., et al. (2019). Genetic characterization of maize germplasm derived from Suwan population and temperate resources. *Hereditas* 156, 1–8. doi: 10.1186/s41065-018-0077-1

Xu, J., Liu, Y., Liu, J., Cao, M., Wang, J., Lan, H., et al. (2012). The genetic architecture of flowering time and photoperiod sensitivity in maize as revealed by QTL review and meta-analysis. *J. Integr. Plant Biol.* 54, 358–373. doi: 10.1111/j.1744-7909.2012.01128.x

Yang, Q., Li, Z., Li, W., Ku, L., Wang, C., Ye, J., et al. (2013). CACTA-like transposable element in ZmCCT attenuated photoperiod sensitivity and accelerated the postdomestication spread of maize. *PNAS* 110, 16969–16974. doi: 10.1073/pnas.1310949110

Zhang, Z., Li, X., Zhang, C., Zou, H., and Wu, Z. (2016). Isolation, structural analysis, and expression characteristics of the maize nuclear factor Y gene families. *Biochem. Biophys. Res. Commun.* 478, 752–758. doi: 10.1016/j.bbrc.2016.08.020

Zhang, X., Tang, B., Liang, W., Zheng, Y., and Qiu, F. (2011). Quantitative genetic analysis of flowering time, leaf number and photoperiod sensitivity in maize (*Zea mays* L.). *J. Plant Breed. Crop Sci.* 3, 168–184.

Zhao, Z., Chen, T., Yue, J., Pu, N., Liu, J., Luo, L., et al. (2023). Small Auxin Up RNA 56 (SAUR56) regulates heading date in rice. *Mol. Breed.* 43, 62. doi: 10.1007/s11032-023-01409-w

Zhu, L., Guan, Y., Liu, Y., Zhang, Z., Jaffar, M. A., Song, A., et al. (2020). Regulation of flowering time in chrysanthemum by the R2R3 MYB transcription factor CmMYB2 is associated with changes in gibberellin metabolism. *Hortic. Res.* 7, 1–10. doi: 10.1038/s41438-020-0317-1